PRIMARY RESEARCH PAPER

Intermediate-size cell dominance in the phytoplankton community of an eutrophic, estuarine ecosystem (Guadalhorce River, Southern Spain)

Jorge J. Montes-Pérez · Enrique Moreno-Ostos · Emilio Marañón ·
José María Blanco · Valeriano Rodríguez · Jaime Rodríguez

Abstract The size–abundance spectrum (SAS) of phytoplankton is controlled by the interplay of physical and biological factors whose particular relevance varies between ecosystems. Here we report the results of a study of phytoplankton SAS in a system of eight estuarine shallow, eutrophic lagoons (Guadalhorce river, South Spain). SAS were obtained through a combination of flow cytometry and image analysis microscopy techniques covering six orders of magnitude from picoplankton to microplankton. Cell numbers were classified into a log2 scale of cell volume to model the log–log relation between cell abundance (cells/mL) and cell volume (μm^3). The resulting averaged phytoplankton SAS can be described by a log–log transformed, power model with a slope of -0.62 (that is, there is an allometric relation between the size and abundance of cells). The distribution of biovolume ($\mu m^3/l$) in broader size categories is characterized by the dominance of nanoplankton (67.4%), followed by microplankton (30.1%) and picoplankton (2.5%). The minor relative contribution of picoplankton to total biovolume can be explained by a combination of high and variable rates of nutrient inputs, light stress and grazing. The biomass dominance of intermediate-size cells (nanoplankton) is coherent with experimental findings describing the unimodal size scaling of growth rate, with maximum values centered in this size category.

Keywords Phytoplankton · Intermediate-size cell · Eutrophic · Estuary · Size–abundance spectra

Introduction

Many phytoplankton physiological and ecological processes (such as metabolic rates, light absorption, nutrient uptake, sinking rates, and susceptibility to grazing) are strongly determined by cell size (Fenchel, 1974; Calder, 1983; Peters, 1983; Chisholm, 1992; Marañón, 2015). As a consequence, the size structure of phytoplankton communities is closely related to numerous ecosystem properties, including food-web organization, energy flow, matter cycling and stability (Platt & Denman, 1977; Peters, 1983; Rodríguez & Li, 1994; Gaedke et al., 2004; Acevedo-Trejos et al., 2015; Moreno-Ostos et al., 2015).

Measurement of the amount of chlorophyll within different size classes through fractionation methods

J. J. Montes-Pérez (✉) · E. Moreno-Ostos ·
J. M. Blanco · V. Rodríguez · J. Rodríguez
Marine Ecology and Limnology Research Group,
Department of Ecology and Geology, University of
Málaga, Campus Teatinos S/N, 29071 Málaga, Spain
e-mail: jmontesp@uma.es

E. Marañón
Department of Ecology and Animal Biology, University
of Vigo, 36310 Vigo, Spain

provides a first approximation to the size structure of phytoplankton. However, a more precise approach is based on modeling size–abundance spectra (SAS) (Platt & Denman, 1977; Rodríguez & Mullin, 1986), which describes cell abundance as a mathematical function of cell size (both scales log-transformed). Modeling SAS has led to the consideration of this approach as a valuable tool for the analysis of aquatic ecosystems and is on the basis of several theoretical models on ecological features such as flow of biomass or ecosystem metabolism (Platt et al, 1984; Geider et al., 1986; Cózar et al., 2003; Brown et al., 2004; Gaedke et al., 2004; Glazier, 2009; Marañón, 2009). In addition to this, the size structure of planktonic communities can contribute to the management of aquatic ecosystems. Size–abundance models and parameters can be used as a sensor for different anthropogenic pressures on aquatic ecosystem from the global (e.g., climate change) to the local (e.g., nutrients input or the introduction of exotic species) scales. As a matter of fact, the European Water Framework Directive proposes phytoplankton community composition, species abundance, and frequency and intensity of blooms as elements for phytoplankton-based ecological quality assessment in coastal and transitional waters. However, phytoplankton communities in transitional waterbodies frequently depicts a marked spatial and temporal variability, which makes ecological characterization based on phytoplankton taxonomic features even more complicated (Lugoli et al., 2012). In this context, there is a need for the development of complementary ecological status indicators based on non-taxonomic criteria, including biomass distribution along cell size classes (Garmendia et al., 2011). To make these application possible and useful, it is worthy to previously achieve a solid knowledge about the shape of the size-distribution model and the factors controlling it.

Phytoplankton communities in the oligotrophic ocean show rather linear SAS with a slope value around − 1 (they tend to be isometric), which can be considered as a conservative ecosystem property (Cavender-Bares et al., 2001; Quiñones et al., 2003; Huete-Ortega et al., 2010, 2012; Moreno-Ostos et al., 2015). On the other side, coastal and other productive ecosystems are usually described by allometric models with less negative slope values or non-linear distributions (Rodríguez et al., 1998; Rodríguez et al.,

2001; Rodríguez et al., 2002; Huete-Ortega et al., 2014). Slope variability is even more relevant when considering the phytoplankton SAS of continental aquatic ecosystems (Sprules & Munawar, 1986; Echevarría et al., 1990; Rojo & Rodríguez, 1994; García et al., 1995), where external perturbations and physical forcing promote frequent and sometimes intense fluctuations and variability in rates of nutrient input. This is especially evident in the case of lagoons and shallow lakes, where SAS tend to be more irregular, bumpy and particularly fluctuating (Echevarría et al., 1990; Quintana et al., 2002; Gaedke et al., 2004).

The quantitative analysis of abundance of different size categories suggest that, in productive ecosystems (coastal and upwelling marine waters, estuaries, eutrophic and shallow lakes, reservoirs, etc.) the contribution of picoplankton (cells smaller than 2 μm Equivalent Spherical Diameter, ESD; Sieburth et al., 1978) to total phytoplankton biomass is small compared to that of larger nanoplankton (2–20 μm ESD) and microplankton (> 20 μm ESD) (Chisholm, 1992; Rodríguez et al., 1998; Rodríguez et al., 2002; Huete-Ortega et al., 2014). The usual explanations are (1) that large-size cells would have competitive advantage over smaller size ones due to their higher storage capacity, which permits to sustain high uptake rates for longer periods of time and (2) that small cells suffer a stronger control from grazing, as compared to nano- and microphytoplankton (Kiørboe, 1993; Irigoien et al., 2005).

However, Marañón et al. (2013) have experimentally demonstrated that, under nutrient-replete, exponential growth conditions, both large-size and small-size cells sustain lower growth rates than intermediate-size cells. Such a unimodal size scaling of phytoplankton growth would be explained by size-dependent trade-off processes related to taxon-independent, size-related constraints in nutrient uptake, requirement and assimilation (Marañón et al., 2013; Ward et al., 2017). The unimodal size scaling of maximum growth rate supports a purely physiological mechanism to explain the variability in size structure as a function of resource availability, as picophytoplankton would represent a small contribution of total biomass in rich waters mainly because they grow more slowly than larger cells. Furthermore, the unimodal size scaling pattern predicts that, rather than the largest size fraction (e.g., microphytoplankton), intermediate-size

cells (e.g., nanophytoplankton) should dominate environments with high resource availability.

In this paper, we first model the size–abundance spectrum of phytoplankton in a system of eight estuarine, shallow, eutrophic lagoons (Guadalhorce river, South Spain) and then use the continuous model to see how biomass is distributed among discrete size classes: picoplankton, nanoplankton and microplankton (following Sieburth et al., 1978 or "small," "intermediate," and "large" cells (following Marañón et al., 2013). The goal is to examine under natural conditions the experimental results of Marañón et al. (2013) about the dominance of nanoplankton (or intermediate-size cells) where external perturbations and physical forcing promote frequent and sometimes intense fluctuations and variability in rates of nutrient input.

Materials and methods

Study site

The Guadalhorce river estuarine wetland is located near Málaga, South Spain (36°40′23.3″ N, 4°27′20.8″ W). It constitutes a salt marsh area of 67 ha confined between the two Guadalhorce river branches and the Mediterranean shore (Fig. 1). After years of anthropic use, the wetland underwent an intense hydrological and ecological rehabilitation as waterbirds habitat, and at the present time it is formed by ten permanent shallow lagoons. To attend to the conservation of its biodiversity, the Andalusian Government declared this wetland as a Natural Site ("Paraje Natural"), a very restrictive protection figure for ecosystems with a high environmental value.

For this study, we selected eight lagoons (Fig. 1) with surfaces ranging from 1500 to 67,000 m^2 and average depth around 0.5 m. A total of 11 one day surveys were carried out from October 2015 to January 2017 covering all seasons (Fig. 2). In each sampling, all lagoons were sampled early in the morning.

Physical and chemical variables, nutrients concentration and chlorophyll a concentration

Due to the reduced surface and shallowness of the studied lagoons, water samples, and physical and chemical data were collected from the littoral zone some meters away from the shore, avoiding any contact with the sediment. Dissolved oxygen concentration, water temperature, salinity, turbidity, and pH were determined in situ using a Hanna Instruments HI9829 multiparameter probe. Dissolved inorganic nutrients concentration (nitrate, nitrite, ammonium, phosphate, and silicate) were determined on 50-ml filtered (GF/C filter) water samples using a Skalar San + autoanalyzer. Dissolved Inorganic Nitrogen concentration (DIN) was calculated as the sum of nitrate, nitrite and ammonium molar concentrations. Chlorophyll a concentration was determined on 50-ml filtered (GF/C) water samples. Pigments were extracted in 90% acetone and their concentration measured using a Turner Design fluorometer following Smith et al. (1981).

Trophic state evaluation

To assess the trophic status of each lagoon, the trophic index TRIX (Vollenweider et al., 1998) was calculated from the mean concentration of dissolved nutrients, chlorophyll a and dissolved oxygen as

$$\text{TRIX} = \left[\log\left(PO_4^{3-} \times DIN \times Chl\text{-}a \times D\%O_2\right) + 1.5\right]/1.2$$

where concentrations of PO_4^{3-}, DIN and chlorophyll a are in mg/m^3 and $D\%O_2$ is the % deviation of the oxygen concentration from saturation conditions. TRIX values were classified into the eutrophication ranges provided by Pavlidou et al. (2015).

Cell size and abundance

Cells larger than 20 μm ESD were studied on 250-ml water samples fixed with 1% Lugol's iodine and settled following the Utermöhl method (Lund et al., 1958). Then we used an inverted Leica DMIL microscope fitted with an F-145 Allied Vision camera to count and measure cells. Images were processed using specific and public software developed by one of the authors (J.M. Blanco) at University of Málaga (Fot-O-Matón II). Length and width of at least 100 cells/colonies were measured for the different phytoplankton geometric shapes (Hillebrand et al., 1999) present in the samples. Cell volumes were calculated from the obtained morphological data.
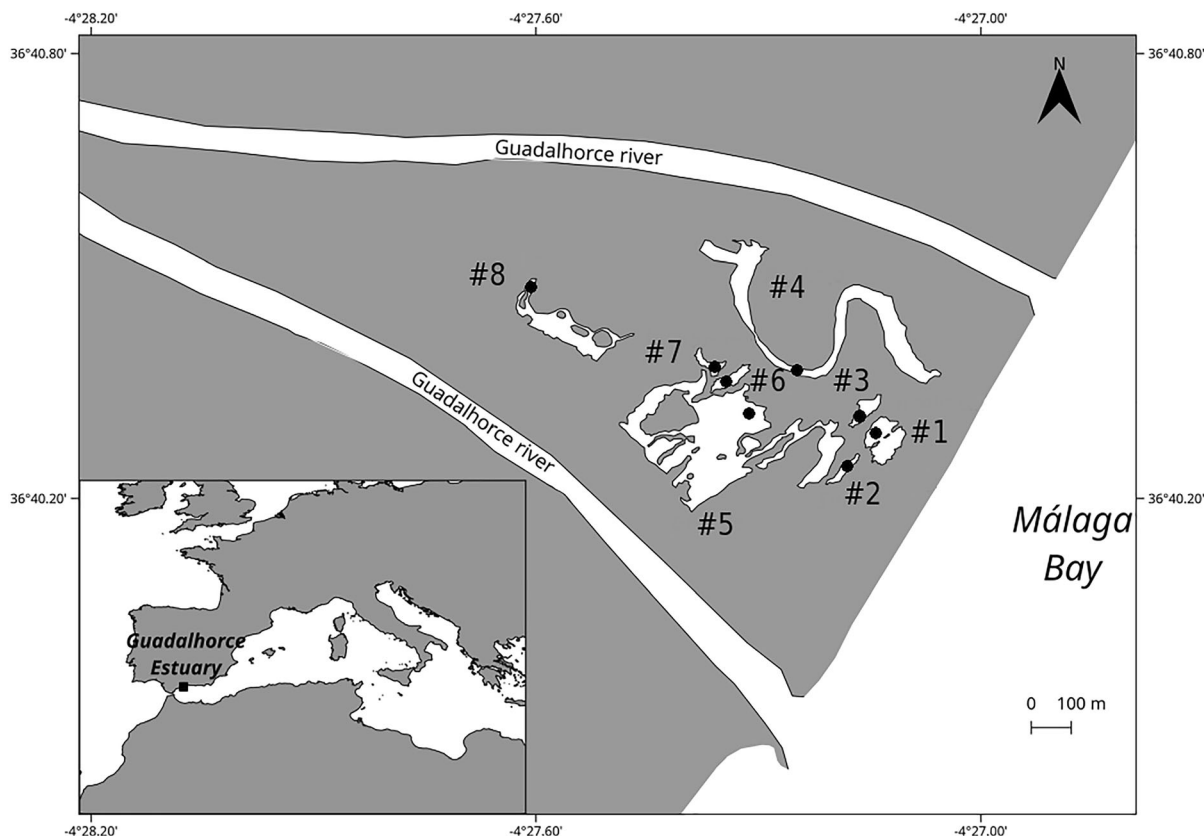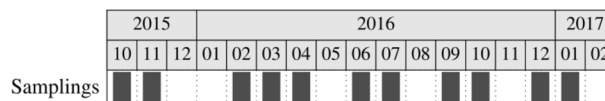
Fig. 1 Location of Guadalhorce river estuary in the Iberian Peninsula (Málaga, South Spain), and detail of the studied lagoons within the coastal wetland. Nomenclature of lagoons (#1, #2,…8#) is linked with a sea-land gradient. Black circles show sampling points

Fig. 2 Sampling schedule showing months in which samplings were carried out

Cells smaller than 20 μm ESD were analyzed on fresh water samples using an Accuri flow cytometer (FC) (Becton Dickinson). To convert FC optical signals to cell volume, the equipment was calibrated with the microscopy image analysis system using the following materials:

(a) Standard flow cytometry size calibration kit (Invitrogen Molecular probes) with non-fluorescent beads (1, 2, 4.2, 6, 10, and 15.4 μm diameter).

(b) Phytoplankton cultures of 7 different species (*Synechococcus oceanicus* W.T.Hall & G.Claus, *Synechococcus* RCC33 C. Nägeli, *Ostreococcus tauri* C.Courties & M.-J.Chrétiennot-Dinet, *Nannochloropsis gaditana* L.M. Lubián, *Isochrysis galbana* Parke, *Rhodomonas salina* (Wislouch) D.R.A.Hill & R.Wetherbee and *Tetraselmis chui* Butcher), covering a range from 0.5 to 52 μm³ cell volume (1 to 4.6 μm ESD).

(c) Several natural samples collected during the studied period, all of them depicting high cell abundance and clearly differentiated flow cytometry signals. Fifteen flow cytometry clusters from natural samples were used in this calibration, with mean cell size ranging from 1.8 to 34,400 μm³ (1.5 to 40 μm ESD) and comprising 5 phytoplankton taxa (Rhodophyta, Miozoa, Chlorophyta, Cyanobacteria, and Euglenozoa). Between 200 and 400 cells were

measured for each flow cytometry cluster. Finally, an exponential regression function between log cell volume and log FSC-H ("Forward Side scatter" signal) was fitted (Fig. 3) to data. Changes in the relationship between FSC-H signal and cell size derived from signal drift (controlled using the FC calibration kit) did not significantly affect calibration during the period of study.

Phytoplankton size–abundance spectra

SAS were built by combining the size–abundance distributions obtained from flow cytometry and microscope image analysis, following the procedure detailed in Moreno-Ostos et al. (2015). We classified cell volume measurements according to an "octave" ($\log_2$) size scale and then analyzed the relationship between the log-transformed values of abundance (cells/ml) and nominal cell volume (μm^3), this being described by the lower limit (equivalent to the amplitude) of each $\log_2$ size class (Blanco et al., 1994).

The use of a $\log_2$ size scale permits to have a rather precise estimation of total biovolume (Bv, $\mu m^3/l$) for any particular size class, since the amplitude of any size class ($2V_i – V_i$) is equal to the lower limit (or nominal size) of the class. Then, Bv (size class V_i to $2V_i$) $= N_i \times V_i$, where N_i is cell abundance in the size class and V_i the nominal cell volume of that size class. From here we calculated total biovolume for the following size categories: picoplankton (0.2–2 μm ESD, nanoplankton (2–20 μm ESD) and microplankton (20–200 μm ESD) following Sieburth et al (1978), and "small" ($< 10^2$ μm^3), "intermediate" (10^2–10^4 μm^3), or "large" ($> 10^4$ μm^3) cells as a derivation from Marañón et al. (2013) and Marañón (2015) observations.

Total biovolume for any size class was then calculated as the sum of biovolumes of the $\log_2$ size classes included within any of these categories. As an example, total biovolume for nanoplankton (cells between 2 and 20 μm ESD) was obtained as

$$Bv(\text{Nanoplankton}) = \sum_{i=2\mu m ESD}^{i=20\mu m ESD} (N_i V_i)$$

Results

Temperature, conductivity and turbidity

Although there is a clear seasonal cycle with temperatures ranging between 10 and 300°C, there were no significant differences among lagoons at any moment during the period of study (Fig. 4a). Water conductivity, however, exhibited a marked land-to-sea gradient, with mean values ranging from 16.7 mS/cm in the innermost lagoon #8 to 128.7 mS/cm in the closest to the sea lagoon #1 (Fig. 4b). Seasonal changes in conductivity values were directly related to water temperature ($r^2 = 0.14$, $n = 88$, $P < 0.001$) through evaporation, the highest values being recorded in summer and the lowest during autumn and winter. The only exception was lagoon #8, where low conductivity remained stable throughout the study period.

Turbidity exhibited high inter- and intra-lagoon variability, with values ranging between 5.3 and 80.7 FNU (Table 1). Following the empirical expressions by Koenings & Edmundson (1991), those turbidity values should roughly correspond to light extinction coefficients between 0.8 and 7.6 m^{-1}. Taking into account that the mean depth of these lagoons is around 0.5 m, it could be concluded that the photic layer extends to the bottom during most of the year in these ecosystems.
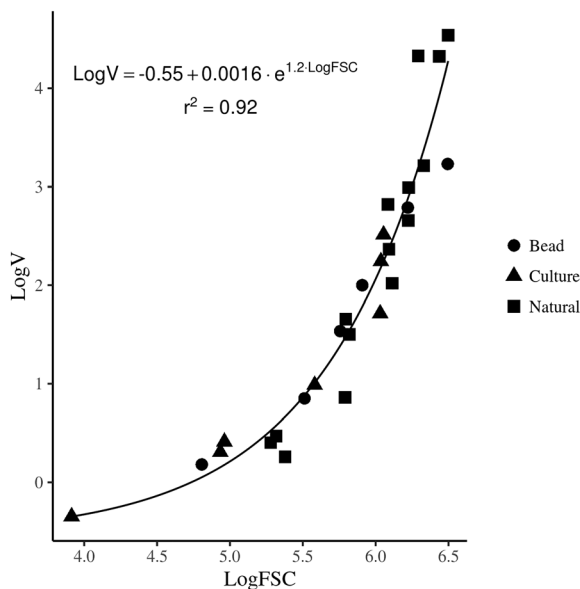

$$LogV = -0.55 + 0.0016 \cdot e^{1.2 \cdot LogFSC}$$
$$r^2 = 0.92$$

Fig. 3 Relationship between cell volume (μm^3) and flow cytometry forward side scatter signal (FSC-H)
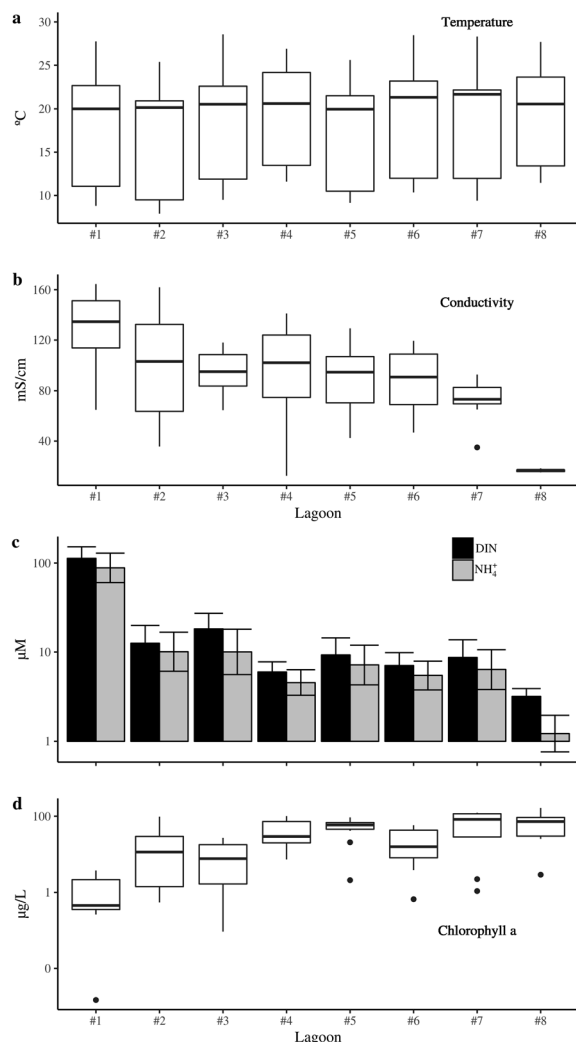
Fig. 4 Physical and chemical variables and chlorophyll a concentration recorded during studied period for each lagoon. Abscissas for dissolve inorganic nitrogen (DIN), ammonia and chlorophyll a are represented in log$_{10}$ scale. Horizontal lines in boxplots (**a**, **b**, **d**), represent median values, the lower and upper hinges correspond to the first and third quartiles and the upper and the lower whiskers extend from the hinge to the largest or the smallest value no further than 1.5 Points are outliers. In barplot (**c**) is represented mean values and standard deviation

Dissolved inorganic nutrients

Dissolved Inorganic Nitrogen concentration (DIN) showed a decreasing gradient of concentration toward the interior of the estuary, with values ranging between a maximum of 379.4 µM in closest to the sea lagoon #1 and a minimum of 1.2 µM in innermost lagoon #8 (Fig. 4c). The gradient is driven by

ammonium concentration, which was 1–2 orders of magnitude higher than nitrate concentration and represented more than 90% of DIN close to the coast (lagoons #1, #2) and less than 70% in the innermost lagoon #8 (Fig. 4c). We did not observe a clear gradient of phosphate concentration, with values ranging between 0.79 µM in lagoon #8 and 2.71 µM in lagoon #7 (Table 1).

Chlorophyll *a* and total phytoplankton biovolume

There is a positive and significant relation between chlorophyll *a* concentration and total phytoplankton biovolume ($r^2 = 0.51$, $P < 0.001$, $n = 88$), both properties showing an increasing gradient of concentration toward the interior of the estuary. Mean values of chlorophyll concentration ranged between 1.3 and 64 µg/l (Fig. 4d), whereas phytoplankton biovolume ranged between 1.15×10^7 and 2.27×10^8 µm^3/ml.

Trophic status

During the studied period, the eight coastal lagoons showed mean TRIX index values higher than 5.3, which corresponds to highly eutrophized coastal ecosystems (Pavlidou et al., 2015). The average TRIX value in the wetland was 7.72 ± 0.61 (Table 1).

Phytoplankton size–abundance distribution

Cell size range analyzed extends from 0.6 to 125 µm ESD (1 to 10^6 µm^3), thus covering six orders of magnitude in terms of cell volume, including picoplankton, nanoplankton, and microplankton. The averaged size–abundance spectrum of phytoplankton (Fig. 5) is continuous along the complete size range observed and can be described by the allometric model $\log (N) = 4.9 - 0.62 \log (V)$ ($r^2 = 0.95$).

Using the classical Sieburth's categories, nanoplankton shows the highest biovolume (Fig. 6a), followed by microplankton and picoplankton. We have also calculated total biovolume for size categories identified as "small" ($< 10^2$ µm^3), "intermediate" (10^2–10^4 µm^3), and "large" ($> 10^4$ µm^3) size cells with a very similar result, that is, the consistent dominance of intermediate-size cells (Fig. 6b).

Table 1 Physical and chemical and biological variables recorded for each studied lagoon

Lagoon	NO_3^-	NO_2^-	NH_4^+	SRP	FNU	D.O	TRIX
#1	10.6 ± 25.1	3.1 ± 2.7	138.7 ± 103.9	1.6 ± 1.2	5.3 ± 3.4	5.7 ± 2.9	6.7 ± 1.2
#2	1.3 ± 1.1	0.4 ± 0.2	37.4 ± 60.9	1 ± 0.6	26 ± 33.4	5.8 ± 2.8	6.8 ± 0.9
#3	4.2 ± 7.8	1.4 ± 1.5	30.2 ± 44.6	1.1 ± 1	5.6 ± 5.8	6.2 ± 3.9	6.9 ± 1
#4	0.7 ± 0.4	0.4 ± 0.3	7.9 ± 9.8	1.1 ± 0.7	23.7 ± 14.4	5.9 ± 4.8	7.2 ± 0.8
#5	1.3 ± 1.5	0.4 ± 0.3	30.3 ± 44.6	2.1 ± 2.3	80.7 ± 86.7	6.8 ± 3.6	7.6 ± 0.6
#6	1 ± 1	0.3 ± 0.3	12.2 ± 21	1 ± 0.7	27 ± 36.8	7.4 ± 2.6	6.8 ± 0.7
#7	1.7 ± 3	1.3 ± 3	36.6 ± 93.1	2.7 ± 4.4	21 ± 14.2	9.6 ± 4.1	7.6 ± 0.6
#8	1 ± 0.6	0.3 ± 0.4	2.8 ± 3.5	0.8 ± 0.5	14.6 ± 9.8	5.5 ± 1.9	7.2 ± 0.5

Nitrate (NO_3^-), nitrite (NO_2^-), ammonia (NH_4^+) and soluble reactive phosphorous (SRP) concentrations are expressed in μM, temperature in °C, turbidity in FNU, conductivity in mS/cm, Chlorophyll a in μg/l, dissolved oxygen in mg/l and trophic status index in relative units. Values show mean ± standard deviation for the whole studied period

Fig. 5 Averaged size–abundance spectra combining all measurements from all lagoons and sampling dates for the entire studied period. Points and bars are mean abundance and standard deviation, respectively, in each size class. Second x axis illustrates cell sizes represented as equivalent spherical diameter
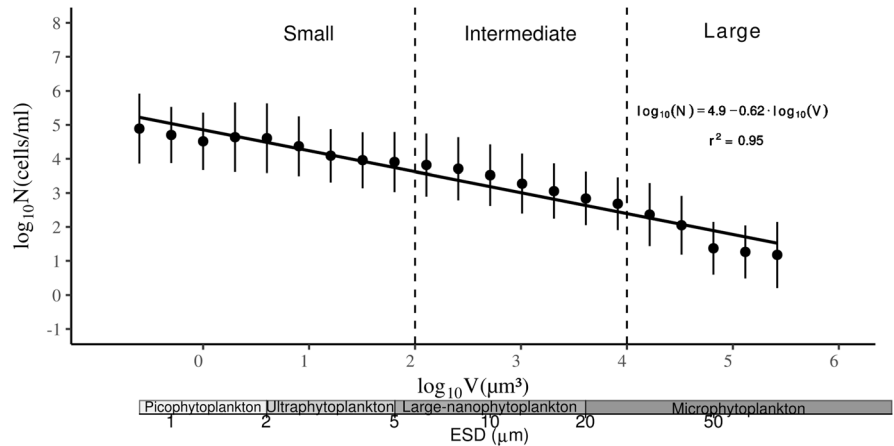
Discussion

Trophic status of the Guadalhorce lagoons

Mediterranean estuarine lagoons are among the most vulnerable and least studied estuarine ecosystems worldwide (Kennison & Fong, 2014). The intense anthropic use of Mediterranean coastal areas and associated watershed modifications typically results in severe nutrient enrichment and eutrophication. In this context, our estuarine lagoons system showed high TRIX values and can be identified as a highly eutrophized ecosystems following Pavlidou et al. (2015), with particularly high concentrations of ammonium, which accounts for more than 85% of total dissolved inorganic nitrogen.

Such high ammonium concentration could be driven by agriculture and wastewater anthropogenic loading as well as to microbial dissimilatory nitrate reduction to ammonia (DNRA) in the presence of organic matter under reducing conditions (Gilbert et al., 2013). A recent study on sediment cores in five of the Guadalhorce lagoons (Gutiérrez Parejo, 2017) demonstrates that their sediment–water interface constitutes a reducing environment with high levels of organic matter, particularly in the lagoons closer to the coast, which is in agreement with our observations about ammonium availability (Fig. 4c). This biogeochemical process could be enhanced by the degradation of the dense adjacent marshes, which supply organic matter and support reducing environments within the lagoons. In addition to this, the dense waterbird populations that inhabit these lagoons could also contribute to increasing organic matter and ammonium concentration through the guanotrophication process (Leentvaar, 1967; Batanero et al., 2017).

Some preliminary results (Conejo-Orosa & Moreno-Ostos, 2018) indicate that both nutrient loads and trophic state in the Guadalhorce lagoons are related to waterbirds abundance and community composition. This would also explain the observed gradient since waterbirds populations depict higher abundances in the lagoons located near the sea shore, where both continental and marine waterfowl species coexist.

In coherence with the eutrophic character of the ecosystem, mean phosphate concentration in most lagoons was higher than 1.1 μM, the threshold concentration for highly eutrophicated transitional and coastal waters proposed by the European Environment Agency (EAA) classification for water quality (Crouzet et al., 1999).

Recorded DIN and phosphate concentrations were always higher than the threshold values proposed for potential nutrient limitation by Ryding & Rast (1992), Justić et al. (1995a, b), Maberly et al. (2002), and Reynolds (2006), so it could be concluded that no nutrient limitation actually occurred in these lagoons during the study period.

Factors controlling phytoplankton size structure

The size–abundance spectrum model of phytoplankton is allometric, showing a slope of − 0.7 which clearly differs from the well-known linear size spectra with slopes around − 1 (or even more negative) typically described in oligotrophic, open ocean, pelagic ecosystems (Rodríguez & Mullin, 1986; Moreno-Ostos et al., 2015). Slope values flatter than − 1 are usual in productive ecosystems both marine and freshwater (Rojo & Rodríguez, 1994; Huete-Ortega et al., 2014).

Although the size structure of the community can be described by a linear model, data points distribution is slightly bumpy (Fig. 4). Departure from linearity has been described in "frequently perturbed," stressed aquatic ecosystems, such as marine polar ecosystems (Witek & Krajewska-Soltys, 1989; Rodríguez et al. 2002), Mediterranean high mountain lakes (Echevarría et al., 1990; Rodríguez et al., 1990), lakes with extreme environmental conditions (Gasol et al., 1991; Steinberg et al., 1998a, b), shallow eutrophic lakes (García et al., 1995; Cózar et al., 2003; Gaedke et al., 2004) and coastal lagoons (Quintana et al., 2002; Thomas et al., 2005; Sousa et al., 2007). In this context, García et al. (1995) conclude that small,

shallow, saline, and eutrophic ecosystems typically show a higher variability in SAS and a more uneven biomass distribution, and Cózar et al. (2003) find that total irregularity in the SAS of a set of subtropical shallow lakes increased with trophic status. In any case, although being bumpy and flatter, phytoplankton SAS in the Guadalhorce estuarine lagoons show a continuous distribution of phytoplankton abundance along the complete size range during the whole study period. According to Gaedke et al. (2004), this continuity indicates that all potential niches are filled and has been interpreted as a continuum of functional guilds, a feature of highly developed food webs (Gaedke, 1992; Cózar et al., 2003).

The distribution of biomass by size depends on physiological factors related with nutrient uptake, biomass production and growth but also on loss processes such as predation, viral lysis, UV damage, sinking and resuspension, among other factors, all of which can be subject to various degrees of size dependence. The bumpy distribution of data points around the regression line (Fig. 5) results in the higher contribution of intermediate-size cells (nanoplankton) to total phytoplankton biomass in comparison with that of microphytoplankton and picoplankton (Fig. 6a), the latter representing less than 5% of total phytoplankton biomass.

There is ample evidence for the low relative contribution of picoplankton biomass in eutrophic ecosystems where nutrient supply is highly intermittent (Rojo & Rodríguez, 1994; Takamura & Nojiri, 1994; Sommaruga & Robarts, 1997; Agawin et al., 2000; Bell & Kalff, 2001; Burns & Galbraith, 2007). This decline in relative picophytoplankton biomass in more productive waters can also be reflected in an equivalent decline in their contribution to primary production in inland and marine ecosystems (Agawin et al., 2000; Bell & Kalff, 2001; Marañón et al., 2012).

Grazing pressure by heterotrophic flagellates (Callieri, 2008) could also contribute to the low biomass of picoplankton, favoring larger-size cells in the competence for nutrients and light (Bell & Kalff, 2001; Burns & Galbratih, 2007). In this context, Schapira et al. (2010) found that picoplankton growth was tightly controlled by fast-growing protozoans under high nutrient conditions in a South Australian coastal lagoon. In agreement, previous studies have shown that picoplankton predominates in hypersaline lakes when heterotrophic nanoflagellates were absent
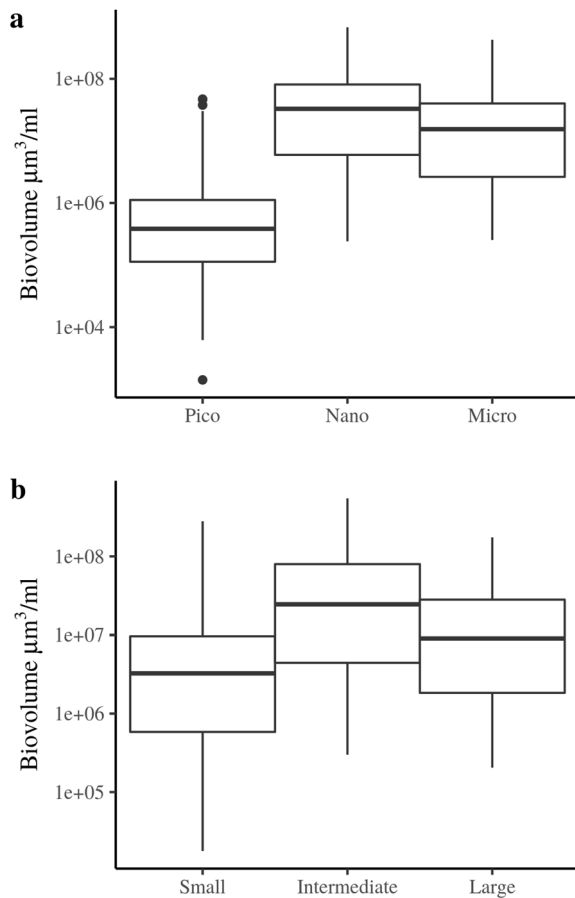
Fig. 6 Phytoplankton biovolume recorded during period studied for each size category. (**a**) Total biovolume for Sieburth's categories: "picoplankton" (< 4.2 μm³), "nanoplankton" ($4.2–4.2 \times 10^3$ μm³), and "microplankton" ($> 4.2 \times 10^3$ μm³). (**b**) Total biovolume for size categories: "small" ($1–10^2$ μm³), "intermediate" ($10^2–10^4$ μm³), and "large" ($10^4–10^6$ μm³) size cells. Horizontal line represents median values, the lower and upper hinges correspond to the first and third quartiles and the upper and the lower whiskers extend from the hinge to the largest or the smallest value no further than 1.5. Point are outliers

(Somogyi et al., 2014). Preliminary analyses show that heterotrophic nanoflagellates were present in the Guadalhorce lagoons, with mean abundances of around 10^3 cells/ml (*data not shown*), typical for temperate inland aquatic ecosystems (Segovia et al., 2016). Additionally, it has been demonstrated that *Artemia* sp., a very common crustacean in the Guadalhorce lagoons, also graze heavily on *Picocystis* cells, a pico-like phytoplankter with 1–3 μm ESD (Roesler et al., 2002).

Some physical characteristics of the lagoons might also help to explain the observed comparatively low contribution of picoplankton to total phytoplankton biomass. Burns & Galbraith (2007) find an inverse and significant relationship between the contribution of picoplankton to total biomass and lake depth, with lowest contribution in shallow lakes. These authors show that the contribution of picoplankton to total microbial biomass comprised $< 1\%$ in estuaries and shallow lakes, while this contribution was significantly higher in reservoirs (7.1%) and deep lakes (16.5%). In this context, Bell & Kalff (2001) suggest that depth could play a complementary role to trophic status influencing the size–abundance structure of phytoplankton communities. These authors also suggest that the frequent recruitment of nano- and microplankton cells by wind-induced sediment resuspension events would explain the inverse relation between picoplankton contribution to phytoplankton biomass and depth. In any case, it is difficult to separate the role of depth from that of the input of nutrients. Since small water bodies tend to receive (per unit volume) more nutrients from the environment, the metabolism of coastal ecosystems like estuaries accelerates with decreasing water body size (Nidzieko, 2018).

It has also been argued that the small size of picoplankton could be a disadvantage in environments exposed to high solar radiation as these small organisms find it difficult to accommodate within their cells sufficient photoprotective substances to avoid visible and ultraviolet radiation damage and photoinhibition (García-Pichel, 1994; Raven et al., 2005; Llabrés & Agustí, 2006; Agustí & Llabrés, 2007; Finkel et al., 2010; Moreno-Ostos et al., 2011). Under high irradiance levels, pico-sized cells typically show increased metabolic cost of screening out damaging radiation (Raven et al., 2005), which results in low growing rates. Llabrés & Agustí (2006) demonstrated that picoplankton from the surface of the Atlantic Ocean is severely affected by exposure to ambient levels of visible and ultraviolet radiation, inducing abrupt cell mortality. Rojo et al. (2012) reported that increased UV radiation in a Central Spanish lake results in picoplankton lower growth rate, biomass and contribution to total phytoplankton biomass. By contrast, nano- and microplankton show a higher package effect, lower susceptibility to photoinhibition and better metabolic performance under high irradiance

levels (Hashimoto & Shiomoto, 2002; Cermeño et al., 2005; Raven et al., 2005; Finkel et al., 2010; Moreno-Ostos et al., 2011; Rojo et al., 2012; Neale et al., 2014). The Guadalhorce lagoons typically depicted low turbidity waters, with photic zone generally extending to the bottom. Taking into account the high visible and ultraviolet radiation levels recorded in the study area (Aguilera et al., 2003), the average light attenuation coefficients and the shallowness of these water masses, we can hypothesize that picoplankton populations could suffer intense light-induced cell damage and mortality, which could also contribute to the observed low relative biomass of this size category.

On the other side of the size spectrum, microplankton (cells larger than 20 μm ESD in Sieburth's classification) would be expected to be the dominant size class in eutrophic productive ecosystems due to their higher storage capacity, which permits them to fill up more slowly when acquiring nutrients and, consequently, sustain high uptake rates for longer periods of time (Malone, 1980; Stolte & Riegman, 1995; Falkowski & Oliver, 2007; Litchman et al., 2007; Verdy et al., 2009; Marañón et al., 2013). In terms of size–abundance modeling, this corresponds to a log–log, linear model where the slope of the relation between the numerical abundance and cell size is < -1.0 which implies that "biomass per logarithmic size class" increases with body size (Platt & Denman, 1977; Rodríguez & Mullin, 1986; Rodríguez & Li, 1994). Our global SAS (Fig. 5) is described by the model $\log N(V) = 4.9 - 0.62 \log V$, which implies that biomass per size class would increase with a slope $= +0.38$. Thus, our results agree with previous observations about the relative dominance of large *versus* small cells in eutrophic ecosystems. However, in addition to this, what our results are showing is that maximum biomass does not accumulate in the largest size category of microplankton but in the intermediate-size category of nanoplankton. On the other hand, the effect of size-dependent sinking loss of largest cells can be discarded because of turbulence in this shallow water layers. In fact, turbulence would balance sinking losses through cells resuspension from the bottom sediment, a phenomenon that can increase the absolute and relative dominance of very large cells as was demonstrated in marine ecosystems by Reul et al. (2006).

Dominance by intermediate-size cells

Our detailed size-spectrum approach combining flow cytometry and microscopy image analysis permits a more precise analysis of the distribution of phytoplankton biomass by size categories in comparison with classical methods based on size-fractionation of chlorophyll. Results show that nanoplankton (and not microplankton) is the size category dominating biomass distribution in this system of eutrophic lagoons (Fig. 6), a pattern that agrees with previous observations. Wehr (1989) showed that phytoplankton dominance can shift from picoplankton to nanoplankton in nutrient enriched environments (Takamura & Nojiri, 1994), and Bec et al. (2011) found that frequent external perturbations (such as nutrient pulses and turbulent mixing episodes) stimulate fast-growing nanoplankton in Mediterranean coastal lagoons. Caroppo (2000) found that nanoplanktonic flagellates were the dominant phytoplankton group in a Mediterranean brackish lagoon, and Thomas et al. (2005) showed that phytoplankton biomass was governed by nanoplankton in two South African eutrophic estuaries. Bell & Kalff (2001) pointed out that the nanoplankton biomass increases with nutrient richness, whereas the relative importance of picoplankton decreases with increasing nutrient load. In productive estuarine systems (Gobler et al., 2002) and eutrophic coastal lagoons, nanoplankton can constitute the dominant phytoplankton size fraction in terms of abundance and biomass, particularly when ammonia is the major source of dissolved inorganic nitrogen, as nanoplankton has the ability to use, and generally prefer, reduced forms of nitrogen to grow (Bec et al., 2011). As previously discussed, this is the case of the Guadalhorce lagoons, where ammonia is, by far, the major component of DIN.

A more general explanation of these observations derives from the experimental demonstration by Marañón et al (2013) of the unimodal relationship between the maximum growth rate of phytoplankton and cell size. Increasing cell size can have opposite effects on metabolism and growth in small to intermediate species (those with ESDs of approximately 0.6 to 10 μm) and intermediate to large species (those with ESDs of approximately 10 to > 100 μm). In other words, intermediate-size cells around 10^2 μm³ show the highest growth rate, which declines sharply as cells become either smaller or larger. This unimodal

size scaling of phytoplankton growth would arise from taxonomic, size-dependent trade-off processes related to nutrient requirement, acquisition, and use (Marañón, 2015). Large-size cells, although characterized by a high ability to acquire nutrients and a large storage capacity, are limited by the conversion of nutrients into biomass. Conversely, small-size cells are constrained by the rate of maximum nutrient uptake relative to their nutritional requirements (Marañón et al., 2013; Marañón, 2015; Ward et al., 2017). The biomass dominance of intermediate-size cells in the nutrient-rich ecosystem studied here agrees with previous observations indicating that the species dominating the community biomass during intense phytoplankton blooms in coastal, productive waters typically have cell volumes in the range 10–20 μm^3 (Marañón 2015). Intermediate-size cells, thanks to their larger ability to exploit transient conditions of increased nutrient supply, are likely to dominate productive environments and thus play a major role in food webs and biogeochemical cycles.

References

Acevedo-Trejos, E., G. Brandt, J. Bruggeman & A. Merico, 2015. Mechanisms shaping size structure and functional diversity of phytoplankton communities in the ocean. Scientific Reports 5: 8918.

Agawin, N. S. R., C. M. Duarte & S. Agustí, 2000. Nutrient and temperature control of the contribution of picoplankton to phytoplankton biomass and production. Limnology and Oceanography 45: 591–600.

Aguilera, J., M. Victoria de Gálvez, R. Conde, E. Pérez-Rodríguez, B. Viñegla, R. Abdala, M. Segovia, E. Herrera & F. L. Figueroa, 2003. Series temporales de medida de radiación solar ultravioleta y fotosintética en Málaga. Actas Dermo-Sifiliográficas Elsevier Doyma 95: 25–31.

Agustí, S. & M. Llabrés, 2007a. Solar Radiation-induced Mortality of Marine Pico-phytoplankton in the Oligotrophic Ocean†. Photochemistry and Photobiology John Wiley & Sons, Ltd (10.1111) 83: 793–801.

Batanero, G. L., E. León-Palmero, L. Li, A. J. Green, M. Rendón-Martos, C. A. Suttle & I. Reche, 2017. Flamingos and drought as drivers of nutrients and microbial dynamics in a saline lake. Scientific Reports Nature Publishing Group 7: 12173, http://www.nature.com/articles/s41598-017-12462-9.

Bec, B., Y. Collos, P. Souchu, A. Vaquer, J. Lautier, A. Fiandrino, L. Benau, V. Orsoni & T. Laugier, 2011. Distribution of picophytoplankton and nanophytoplankton along an anthropogenic eutrophication gradient in French Mediterranean coastal lagoons. Aquatic Microbial Ecology 63: 29–45.

Bell, T. & J. Kalff, 2001. The contribution of picophytoplankton in marine and freshwater systems of different trophic status and depth. Limnology and Oceanography 46: 1243–1248.

Blanco, J. M., F. Echevarría & C. M. García, 1994. Dealing with size-spectra: some conceptual and mathematical problems. Scientia Marina 58: 17–29.

Brown, J. H., J. F. Gillooly, A. P. Allen, V. M. Savage & G. B. West, 2004. Toward a metabolic theory of ecology. Ecology 85: 1771–1789.

Burns, C. W. & L. M. Galbraith, 2007. Relating planktonic microbial food web structure in lentic freshwater ecosystems to water quality and land use. Journal of Plankton Research 29: 127–139.

Calder, W. A., 1983. Body size, mortality, and longevity. Journal of Theoretical Biology 102: 135–144.

Callieri, C., 2008. Picophytoplankton in freshwater ecosystems: the importance of small-sized phototrophs. Freshwater Reviews 1: 1–28.

Caroppo, C., 2000. The contribution of picophytoplankton to community structure in a Mediterranean brackish environment. Journal of Plankton Research 22: 381–397.

Cavender-Bares, K. K., A. Rinaldo & S. W. Chisholm, 2001. Microbial size spectra from natural and nutrient enriched ecosystems. Limnology and Oceanography 46: 778–789.

Cermeño, P., E. Marañón, J. Rodríguez & E. Fernández, 2005. Large-sized phytoplankton sustain higher carbon-specific photosynthesis than smaller cells in a coastal eutrophic ecosystem. Marine Ecology Progress Series 297: 51–60.

Chisholm, S. W., 1992. Phytoplankton Size Primary Productivity and Biogeochemical Cycles in the Sea. Springer, Boston, MA: 213–237.

Conejo-Orosa, T. & E. Moreno-Ostos, 2018. Estimación de cargas de nutrientes por aves acuáticas en las lagunas costera del paraje natural de la Desembocadura del Guadalhorce (Málaga). I Congreso de Jóvenes Investigadores del Mar.: 335–337.

Cózar, A., C. M. García & J. A. Gálvez, 2003. Analysis of plankton size spectra irregularities in two subtropical shallow lakes (Esteros del Iberá, Argentina). Canadian Journal of Fisheries and Aquatic Sciences 60: 411–420.

Crouzet, P., J. Leonard, S. Nixon, Y. Rees, W. Parr, L. Laffon, J. Bøgestrand & P. Kristensen, 1999. Nutrients in European Ecosystems. European Environmental Agency, Copenhagen, Denmark.

Echevarría, F., P. Carrillo, F. Jiménez, P. Sanchez-Castillo, L. Cruz-pizarro & J. Rodríguez, 1990. The size-abundance distribution and taxonomic composition of plankton in an oligotrophic, high mountain lake (La Caldera, Sierra

Nevada, Spain). Journal of Plankton Research 12: 415–422.

Falkowski, P. G. & M. J. Oliver, 2007. Mix and match: how climate selects phytoplankton. Nature Reviews Microbiology 5: 813–819.

Fenchel, T., 1974. Intrinsic rate of natural increase: the relationship with body size. Oecologia 14: 317–326.

Finkel, Z. V., J. Beardall, K. J. Flynn, A. Quigg, T. A. V Rees & J. A. Raven, 2010. Phytoplankton in a changing world: cell size and elemental stoichiometry. Journal of Plankton Research 32: 119–137.

Gaedke, U., 1992. The size distribution of plankton biomass in a large lake and its seasonal variability. Limnology and Oceanography 37: 1202–1220.

Gaedke, U., A. Seifried & R. Adrian, 2004. Biomass Size Spectra and Plankton Diversity in a Shallow Eutrophic Lake. International Review of Hydrobiology 89: 1–20.

Garcia-Pichel, F., 1994. A model for internal self-shading in planktonic organisms and its implications for the usefulness of ultraviolet sunscreens. Limnology and Oceanography 39: 1704–1717.

García, C. M., F. Echevarría & F. X. Niell, 1995. Size structure of plankton in a temporary, saline inland lake. Journal of Plankton Research 17: 1803–1817.

Gasol, J. M., R. Guerrero, & C. Pedró Alió, 1991. Seasonal variations in size structure and procaryotic dominance in sulfurous Lake Cisó. Limnology and Oceanography 36 (5):860–872.

Garmendia, M., M. Revilla, J. Bald, J. Franco, A. Laza-Martínez, E. Orive, S. Seoane, V. Valencia & Á. Borja, 2011. Phytoplankton communities and biomass size structure (fractionated chlorophyll "a"), along trophic gradients of the Basque coast (northern Spain). Biogeochemistry 106: 243–263.

Geider, R. J., T. Platt & J. A. Raven, 1986. Size dependence of growth and photosynthesis in diatoms: a synthesis. Marine Ecology Progress Series 30: 93–104.

Glazier, D. S., 2009. Metabolic level and size scaling of rates of respiration and growth in unicellular organisms. Functional Ecology 23: 963–968.

Glibert, P. M., T. M. Kana & K. Brown, 2013. From limitation to excess: the consequences of substrate excess and stoichiometry for phytoplankton physiology, trophodynamics and biogeochemistry, and the implications for modeling. Journal of Marine Systems 125: 14–28.

Gobler, C. J., M. J. Renaghan & N. J. Buck, 2002. Impacts of nutrients and grazing mortality on the abundance of Aureococcus anophagefferens during a New York brown tide bloom. Limnology and Oceanography 47: 129–141.

Gutiérrez Parejo, P., 2017. Estudio de la fracción orgánica del sedimento de cinco lagunas costeras de la desembocadura del río Guadalhorce. Encuentros en la Biología X: 243–246.

Hashimoto, S. & A. Shiomoto, 2002. Light utilization efficiency of size-fractionated phytoplankton in the subarctic Pacific, spring and summer 1999: high efficiency of large-sized diatom. Journal of Plankton Research 24: 83–87.

Hillebrand, H., C.-D. Dürselen, D. Kirschtel, U. Pollingher & T. Zohary, 1999. Biovolume calculation for pelagic and benthic microalgae. Journal of Phycology 35: 403–424.

Huete-Ortega, M., P. Cermeño, A. Calvo-Díaz & E. Marañón, 2012. Isometric size-scaling of metabolic rate and the size abundance distribution of phytoplankton. Proceedings of the Royal Society 279: 1815–1823.

Huete-Ortega, M., E. Marañón, M. Varela & A. Bode, 2010. General patterns in the size scaling of phytoplankton abundance in coastal waters during a 10-year time series. Journal of Plankton Research 32: 1–14.

Huete-Ortega, M., T. Rodríguez-Ramos, D. C. López-Sandoval, P. Cermeño, J. M. Blanco, R. L. Palomino, J. Rodríguez & E. Marañón, 2014. Distinct patterns in the size-scaling of abundance and metabolism in coastal and open-ocean phytoplankton communities. Marine Ecology Progress Series 515: 61–71.

Irigoien, X., K. J. Flynn & R. P. Harris, 2005. Phytoplankton blooms: a "loophole" in microzooplankton grazing impact? Journal of Plankton Research 27: 313–321.

Justić, D., N. N. Rabalais & R. E. Turner, 1995a. Stoichiometric nutrient balance and origin of coastal eutrophication. Marine Pollution Bulletin 30: 41–46.

Justić, D., N. N. Rabalais, R. E. Turner & Q. Dortch, 1995b. Changes in nutrient structure of river-dominated coastal waters: stoichiometric nutrient balance and its consequences. Estuarine, Coastal and Shelf Science 40: 339–356.

Kennison, R. L. & P. Fong, 2014. Extreme eutrophication in shallow estuaries and lagoons of California is driven by a unique combination of local watershed modifications that Trump variability associated with wet and dry seasons. Estuaries and Coasts 37: 164–179.

Kiørboe, T., 1993. Turbulence, phytoplankton cell size, and the structure of pelagic food webs. Advances in Marine Biology 29: 1–72.

Koenings, J. P. & J. A. Edmundson, 1991. Secchi disk and photometer estimates of light regimes in Alaskan lakes: effects of yellow color and turbidity. Limnology and Oceanography 36: 91–105.

Leentvaar, P., 1967. Observations in guanotrophic environments. Hydrobiologia 29: 441–489.

Litchman, E., C. A. Klausmeier, O. M. Schofield & P. G. Falkwoski, 2007. The role of functional traits and trade-offs in structuring phytoplankton communities: Scaling from cellular to ecosystem level. Ecology Letters 10: 1170–1181.

Llabrés, M. & S. Agustí, 2006a. Picophytoplankton cell death induced by UV radiation: evidence for oceanic Atlantic communities. Limnology and Oceanography 51: 21–29.

Lugoli, F., M. Garmendia, S. Lehtinen, P. Kauppila, S. Moncheva, M. Revilla, L. Roselli, N. Slabakova, V. Valencia, K. M. Dromph & A. Basset, 2012. Application of a new multi-metric phytoplankton index to the assessment of ecological status in marine and transitional waters. Ecological Indicators 23: 338–355.

Lund, J. W. G., C. Kipling & E. D. Le Cren, 1958. The inverted microscope method of estimating algal numbers and the statistical basis of estimations by counting. Hydrobiologia 11: 143–170.

Maberly, S. C., L. King, M. M. Dent, R. I. Jones & C. E. Gibson, 2002. Nutrient limitation of phytoplankton and periphyton growth in upland lakes. Freshwater Biology 47: 2136–2152.

Malone, T. C., 1980. Algal size. In Morris, I. (ed.), The Physiological Ecology of Phytoplankton. Blackwell, London: 433–465.

Marañón, E., 2009. Phytoplankton size structure. In Steele, J. H., K. K. Turekian & S. A. Thorpe (eds), Encyclopedia of Ocean Sciences. Academic Press, Oxford: 4252–4256.

Marañón, E., 2015. Cell size as a key determinant of phytoplankton metabolism and community structure. Annual Review of Marine Science 7: 241–264.

Marañón, E., P. Cermeño, M. Latasa & R. D. Tadonléké, 2012. Temperature, resources, and phytoplankton size structure in the ocean. Limnology and Oceanography 57: 1266–1278.

Marañón, E., P. Cermeño, D. C. López-Sandoval, T. Rodríguez-Ramos, C. Sobrino, M. Huete-Ortega, J. M. Blanco & J. Rodríguez, 2013. Unimodal size scaling of phytoplankton growth and the size dependence of nutrient uptake and use. Ecology Letters 16: 371–379.

Moreno-Ostos, E., J. M. Blanco, S. Agustí, L. M. Lubián, V. Rodríguez, R. L. Palomino, M. Llabrés & J. Rodríguez, 2015. Phytoplankton biovolume is independent from the slope of the size spectrum in the oligotrophic Atlantic Ocean. Journal of Marine Systems 152: 42–50.

Moreno-Ostos, E., A. Fernández, M. Huete-Ortega, B. Mouriño-Carballido, A. Calvo-Díaz, X. A. G. Morán & E. Marañón, 2011. Size-fractionated phytoplankton biomass and production in the tropical Atlantic. Scientia Marina CSIC Consejo Superior de Investigaciones Científicas 75: 379–389.

Neale, P. J., A. L. Pritchard & R. Ihnacik, 2014. UV effects on the primary productivity of picophytoplankton: biological weighting functions and exposure response curves of *Synechococcus*. Biogeosciences 11: 2883–2895.

Nidzieko, N. J., 2018a. Allometric scaling of estuarine ecosystem metabolism. Proceedings of the National Academy of Sciences of the United States of America National Academy of Sciences 115: 6733–6738.

Pavlidou, A., N. Simboura, E. Rousselaki, M. Tsapakis, K. Pagou, P. Drakopoulou, G. Assimakopoulou, H. Kontoyiannis & P. Panayotidis, 2015. Methods of eutrophication assessment in the context of the water framework directive: examples from the Eastern Mediterranean coastal areas. Continental Shelf Research 108: 156–168.

Peters, R. H., 1983. The Ecological Implications of Body Size. Cambridge University Press, New York.

Platt, T. & K. Denman, 1977. Organisation in the pelagic ecosystem. Helgoländer Wissenschaftliche Meeresuntersuchungen 30: 575–581.

Platt, T., M. Lewis & R. Geider, 1984. Thermodynamics of the pelagic ecosystem: elementary closure conditions for biological production in the open ocean. In Fasham, M. J. R. (ed.), Flows of Energy and Materials in Marine Ecosystems. Springer, Boston: 49–84.

Quiñones, R. A., T. Platt & J. Rodríguez, 2003. Patterns of biomass-size spectra from oligotrophic waters of the Northwest Atlantic. Progress in Oceanography 57: 405–427.

Quintana, X. D., F. A. Comín & R. Moreno-Amich, 2002. Biomass-size spectra in aquatic communities in shallow fluctuating Mediterranean salt marshes (Emporda wetlands, NE Spain). Journal of Plankton Research 24: 1149–1161.

Raven, A., Z. Finkel & A. Irwin, 2005. Picophytoplankton: bottom-up and top-down controls on ecology and evolution. Vie et Milieu 55: 209–215.

Reul, A., M. Muñoz, F. Criado-Aldeanueva & V. Rodríguez, 2006. Spatial distribution of phytoplankton <13 μm in the Gulf of Cádiz in relation to water masses and circulation pattern under westerly and easterly wind regimes. Deep Sea Research Part II: Topical Studies in Oceanography 53: 1294–1313.

Reynolds, C. S., 2006. The Ecology of Phytoplankton. Cambridge University Press, Cambridge.

Rodriguez, J., F. Echevarria & F. Jimenez-Gomez, 1990. Physiological and ecological scalings of body size in an oligotrophic, high mountain lake (La Caldera, Sierra Nevada, Spain). Journal of Plankton Research 12: 593–599.

Rodríguez, J., F. Jiménez-Gómez, J. M. Blanco & F. L. Figueroa, 2002. Physical gradients and spatial variability of the size structure and composition of phytoplankton in the Gerlache Strait (Antarctica). Deep-Sea Research Part II: Topical Studies in Oceanography 49: 693–706.

Rodríguez, J. & W. Li, 1994. The size structure and metabolism of the pelagic ecosystem. Scientia Marina 58: 67–79.

Rodríguez, J. & M. M. Mullin, 1986. Relation between biomass and body weight of plankton in a steady state oceanic ecosystem. Limnology and Oceanography 31: 361–370.

Rodríguez, J., J. Tintoré, J. T. Allen, J. M. Blanco, D. Gomis, A. Reul, J. Ruiz, V. Rodríguez, F. Echevarria & F. Jiménez-Gómez, 2001. Mesoscale vertical motion and the size structure of phytoplankton in the ocean. Nature 410: 360–363.

Rodríguez, J., J. M. Blanco, F. Jiménez-Gómez, F. Echevarría, J. Gil, V. Rodríguez, J. Ruiz, B. Bautista & F. Guerrero, 1998. Patterns in the size structure of the phytoplankton community in the deep fluorescence maximum of the Alboran Sea (southwestern Mediterranean). Deep Sea Research Part I: Oceanographic Research Papers 45: 1577–1593.

Roesler, C. S., C. W. Culbertson, S. M. Etheridge, R. Goericke, R. P. Kiene, L. G. Miller & R. S. Oremland, 2002. Distribution, production, and ecophysiology of *Picocystis* strain ML in Mono Lake, California. Limnology and Oceanography 47: 440–452.

Rojo, C., G. Herrera, M. A. Rodrigo, M. J. Ortíz-Llorente & P. Carrillo, 2012. Mixotrophic phytoplankton is enhanced by UV radiation in a low altitude, P-limited Mediterranean lake. Hydrobiologia 698: 97–110.

Rojo, C. & J. Rodríguez, 1994. Seasonal variability of phytoplankton size structure in a hypertrophic lake. Journal of Plankton Research 16: 317–335.

Ryding, S.-O. & W. Rast, 1992. El control de la eutrofización en lagos y pantanos. https://www.sidalc.net/cgi-bin/wxis.exe/?IsisScript=QUV.xis&method=post&formato=2&cantidad=1&expresion=mfn=000893.

Schapira, M., M.-J. Buscot, T. Pollet, S. C. Leterme & L. Seuront, 2010. Distribution of picophytoplankton communities from brackish to hypersaline waters in a South Australian coastal lagoon. Saline Systems 6: 2.

Segovia, B. T., C. D. Domingues, B. R. Meira, F. M. Lansac-Toha, P. Fermani, F. Unrein, L. M. Lobão, F. Roland, L. F. M. Velho & H. Sarmento, 2016. Coupling between heterotrophic nanoflagellates and bacteria in fresh waters: does latitude make a difference? Frontiers in Microbiology 7: 114.

Sieburth, J. M., V. Smetacek & J. Lenz, 1978. Pelagic ecosystem structure: heterotrophic compartments of the plankton and their relationship to plankton size fractions 1. Limnology and Oceanography 23: 1256–1263.

Smith, R. C., K. S. Baker & P. Dustan, 1981. Fluorometric techniques for the measurement of oceanic chlorophyll in the support of remote sensing. Western Journal of Emergency Medicine 14: 1–10.

Sommaruga, R. & R. D. Robarts, 1997. The significance of autotrophic and heterotrophic picoplankton in hypertrophic ecosystems. FEMS Microbiology Ecology 24: 187–200.

Somogyi, B., L. Vörös, K. Pálffy, G. Székely, C. Bartha & Z. G. Keresztes, 2014. Picophytoplankton predominance in hypersaline lakes (Transylvanian Basin, Romania). Extremophiles 18: 1075–1084.

Sousa, R., S. Dias & C. Antunes, 2007. Subtidal macrobenthic structure in the lower lima estuary, NW of Iberian Peninsula. Annales Zoologici Fennici 44: 303–313.

Sprules, W. G. & M. Munawar, 1986. Plankton size spectra in relation to ecosystem productivity, size, and perturbation. Canadian Journal of Fisheries and Aquatic Sciences 43: 1789–1794.

Steinberg, C. E. W., H. Schäfer & W. Beisker, 1998a. Do acid-tolerant cyanobacteria exist? Acta Hydrochimica et Hydrobiologica 26: 13–19.

Steinberg, C. E. W., H. Schäfer, J. Tittel & W. Beisker, 1998b. Phytoplankton composition and biomass spectra created by flow cytometry and zooplankton composition in mining lakes of different states of acidification. In Geller, W., H. Klapper & W. Salomons W. (eds), Acidic Mining Lakes. Environmental Science. Springer, Berlin: 127–145.

Stolte, W. & R. Riegman, 1995. Effect of phytoplankton cell size on transient-state nitrate and ammonium uptake kinetics. Microbiology 141: 1221–1229.

Takamura, N. & Y. Nojiri, 1994. Picophytoplankton biomass in relation to lake trophic state and the TN:TP ratio of lake water in Japan. Journal of Phycology 30: 439–444.

Thomas, C. M., R. Perissinotto & I. Kibirige, 2005. Phytoplankton biomass and size structure in two South African eutrophic, temporarily open/closed estuaries. Estuarine, Coastal and Shelf Science 65: 223–238.

Verdy, A., M. Follows & G. Flierl, 2009. Optimal phytoplankton cell size in an allometric model. Marine Ecology Progress Series 379: 1–12.

Vollenweider, R. A., F. Giovanardi, G. Montanari & A. Rinaldi, 1998. Characterization of the trophic conditions of marine coastal waters with special reference to the NW Adriatic Sea: proposal for a trophic scale, turbidity and generalized water quality index. Environmetrics 9: 329–357.

Ward, B. A., E. Marañón, B. Sauterey, J. Rault & D. Claessen, 2017. The size dependence of phytoplankton growth rates: a trade-off between nutrient uptake and metabolism. American Naturalist 189: 170–177.

Wehr, J. D., 1989. Experimental tests of nutrient limitation in freshwater picoplankton. Applied and Environmental Microbiology 55: 1605–1611.

Witek, Z. & A. Krajewska-Soltys, 1989. Some examples of the epipelagic plankton size structure in high latitude oceans. Journal of Plankton Research 11: 1143–1155.